Electronic Supplementary Material (ESI) for Physical Chemistry Chemical Physics.

SUPPORTING INFORMATION

Using microgels to control the morphology and optoelectronic properties of hybrid organic-inorganic perovskite films

Chotiros Dokkhan[a], Muhamad Z. Mokhtar[a], Qian Chen[a], Brian R. Saunders[a,*]

[a] *School of Materials, University of Manchester, Manchester, M13 9PL, U.K.*

Nigel W. Hodson[b]

[b] *BioAFM Facility, Faculty of Biology, Medicine and Health, Stopford Building, University of Manchester, Oxford Road, Manchester, M13 9PT, U.K.*

Bruce Hamilton[c]

[c] *Photon Science Institute, University of Manchester, Alan Turing Building, Oxford Road, Manchester, M13 9PL, U.K.*

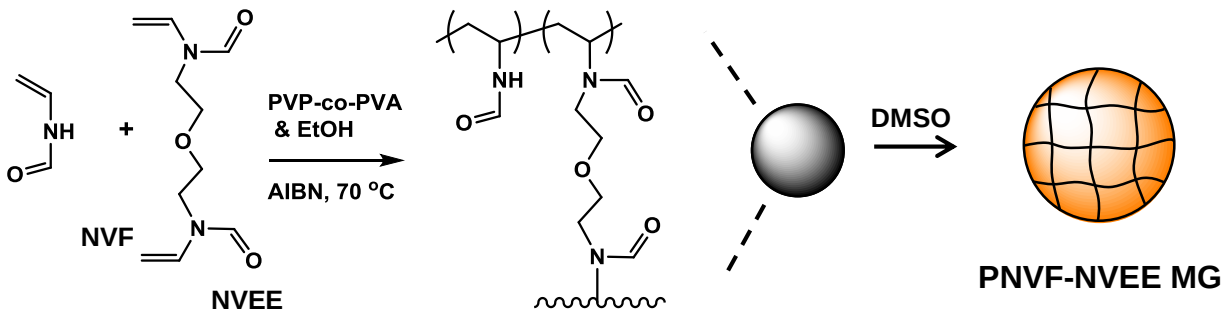

Scheme S1. Depiction of microgel (MG) synthesis using dispersion polymerisation. Details of the synthetic method employed are given in the Experimental section. NVF and NVEE are *N*-vinylformamide and 2-(*N*-vinylformamido)ethyl ether, respectively.

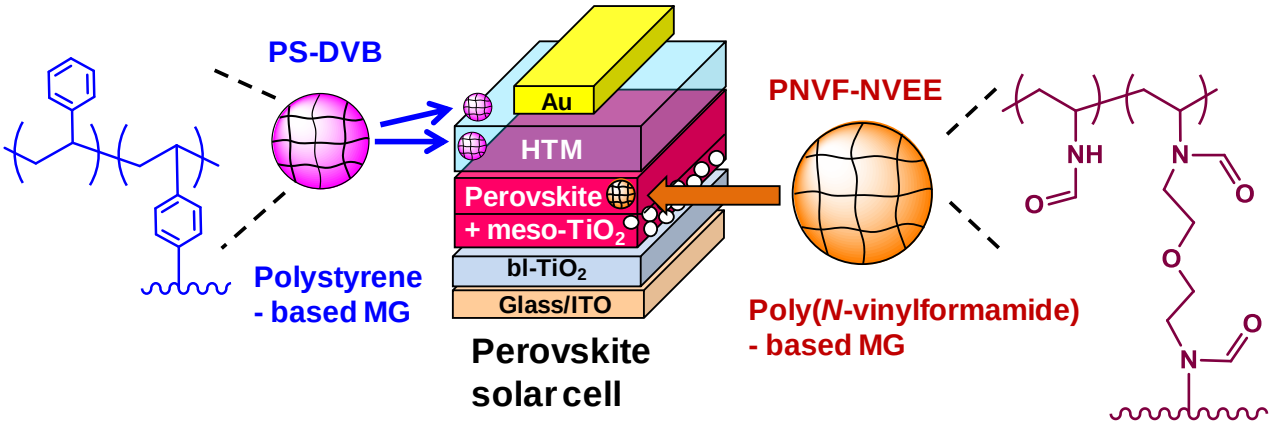

Microgel	Hydrophilic	Hydrophobic	Solvents	PSC use	Ref.
PNVF-NVEE	√	X	DMSO, Water	Perovskite layer micropatterning	This work
PS-DVB	X	√	Toluene, Chlorobenzene	(a) HTM-dilution (b) Encapsulation	1 1

Figure S1. Comparison of the PNVF-NVEE MG used in the present study with the polystyrene (PS) MG used in our previous study[1] for perovskite solar cells (PSCs). DVB (divinylbenzene) and NVEE are crosslinkers. The location within the PSC as well as the structure and properties of the MGs are contrasted in the figure and the table. HTM is the hole transport matrix.

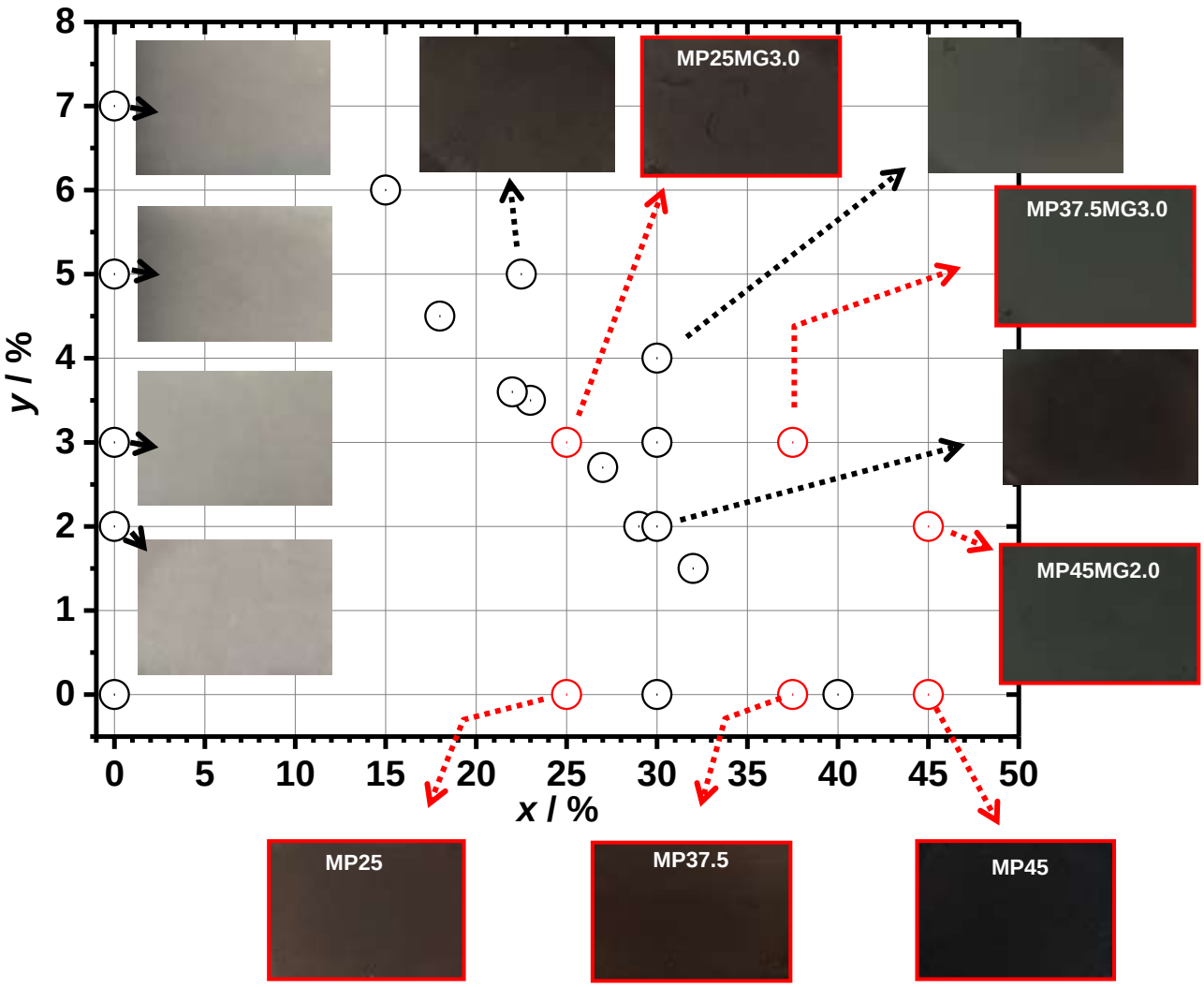

Figure S2. Digital photographs recorded for $MAPbI_{3-z}Cl_z$/MG films (i.e., MP*x*MG*y*) prepared using various solution compositions. The parameters *x* and *y* are the nominal $MAPbI_{3-z}Cl_z$ and MG concentrations used during spin coating. The six films studied in detail are shown in red. The dimensions of the films were 20 mm x 15 mm.

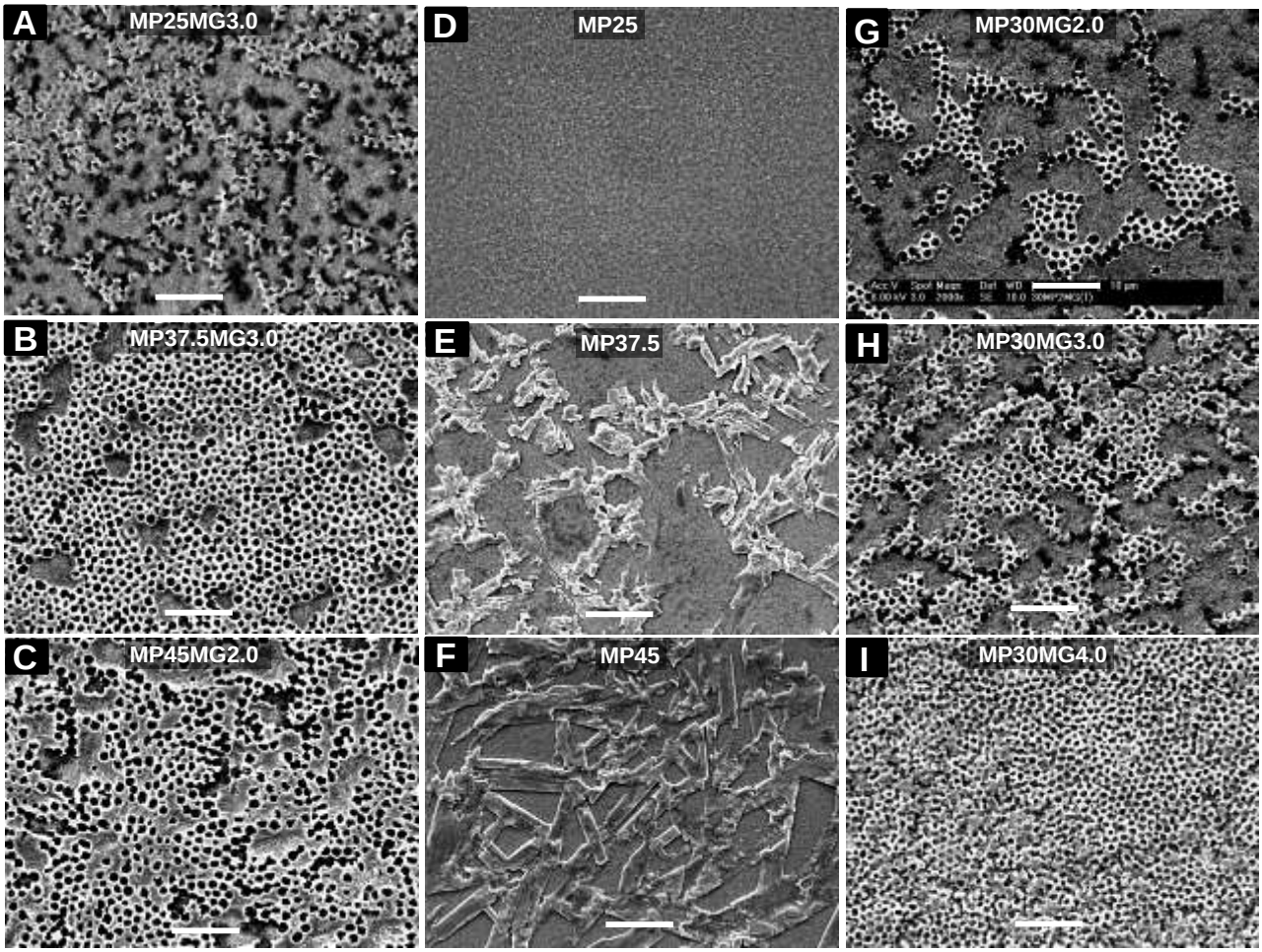

Figure S3. Lower magnification SEM images obtained for (**A**) MP25MG3.0, (**B**) MP37.5MG3.0, (**C**) MP45MG2.0, (**D**) MP25, (**E**) MP37.5 and (**F**) MP45 films. SEM images are also shown for (**G**) MP30MG2.0, (**H**) MP30MG3.0 and (**I**) MP30MG4.0. Scale bars: 10 μm.

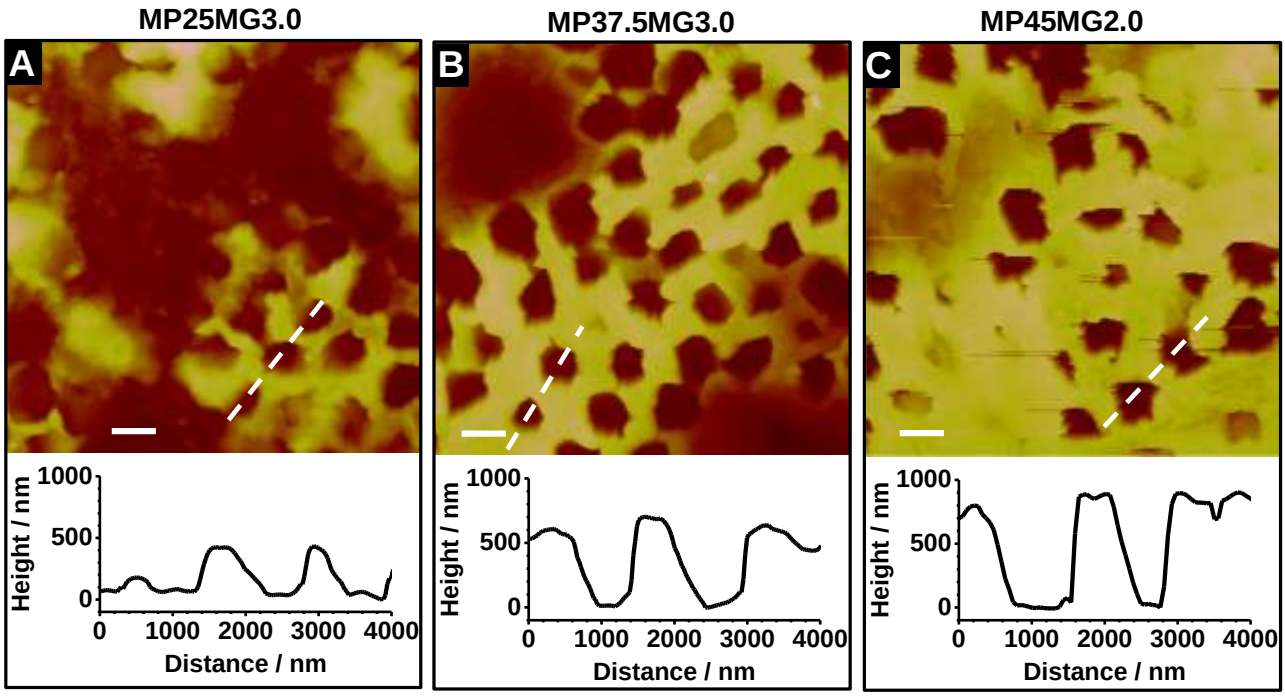

Figure S4. Tapping mode AFM images and line profiles measured for (**A**) MP25MG3.0, (**B**) MP37.5MG3.0 and (**C**) MP45MG2.0 films. The scale bars are 1.0 μm.

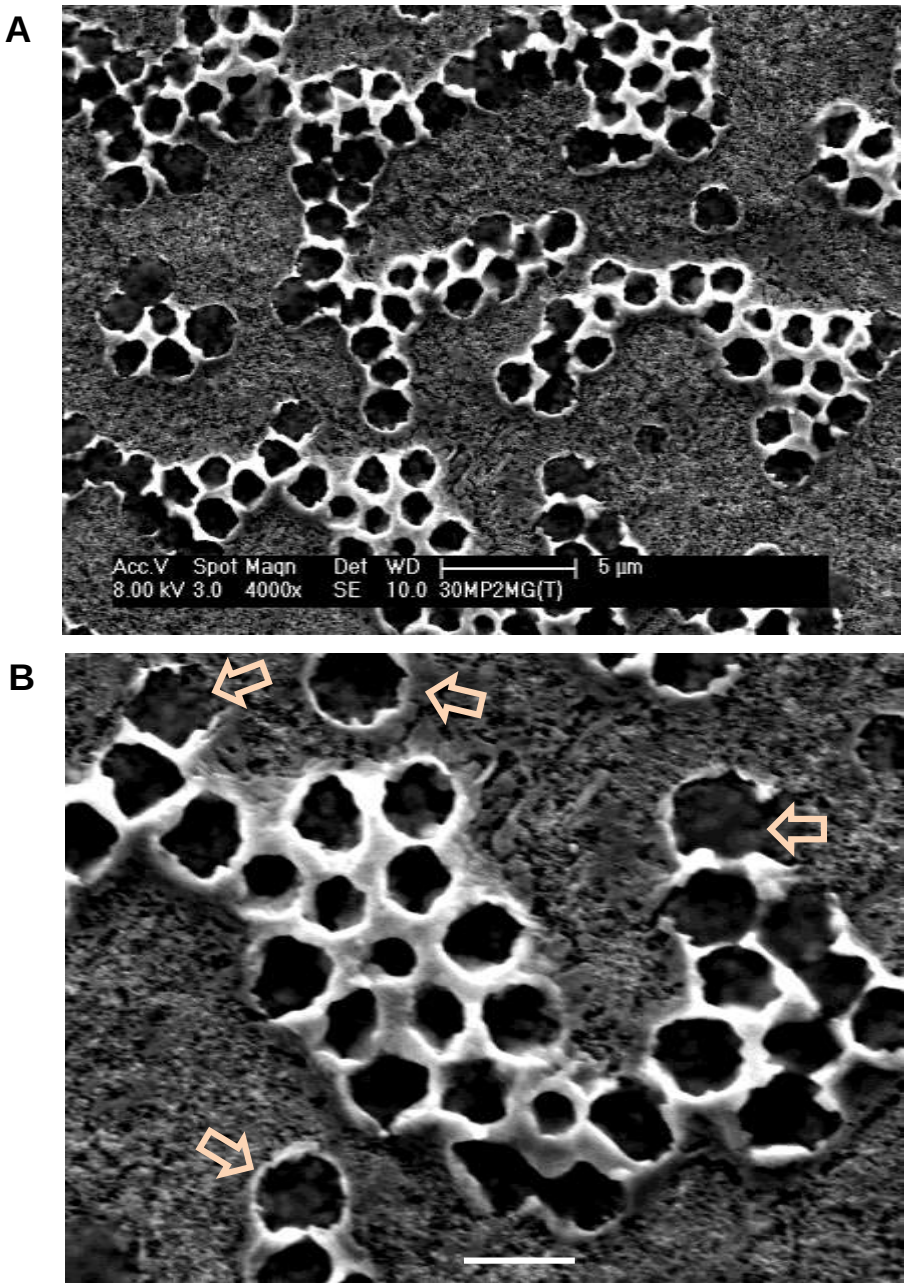

Figure S5. High magnification SEM images for MP30MG2.0. The scale bars in (**A**) and (**B**) are 5.0 and 2.0 μm, respectively. The arrows in (B) highlight enclosed flattened MGs particles within a perovskite wall.

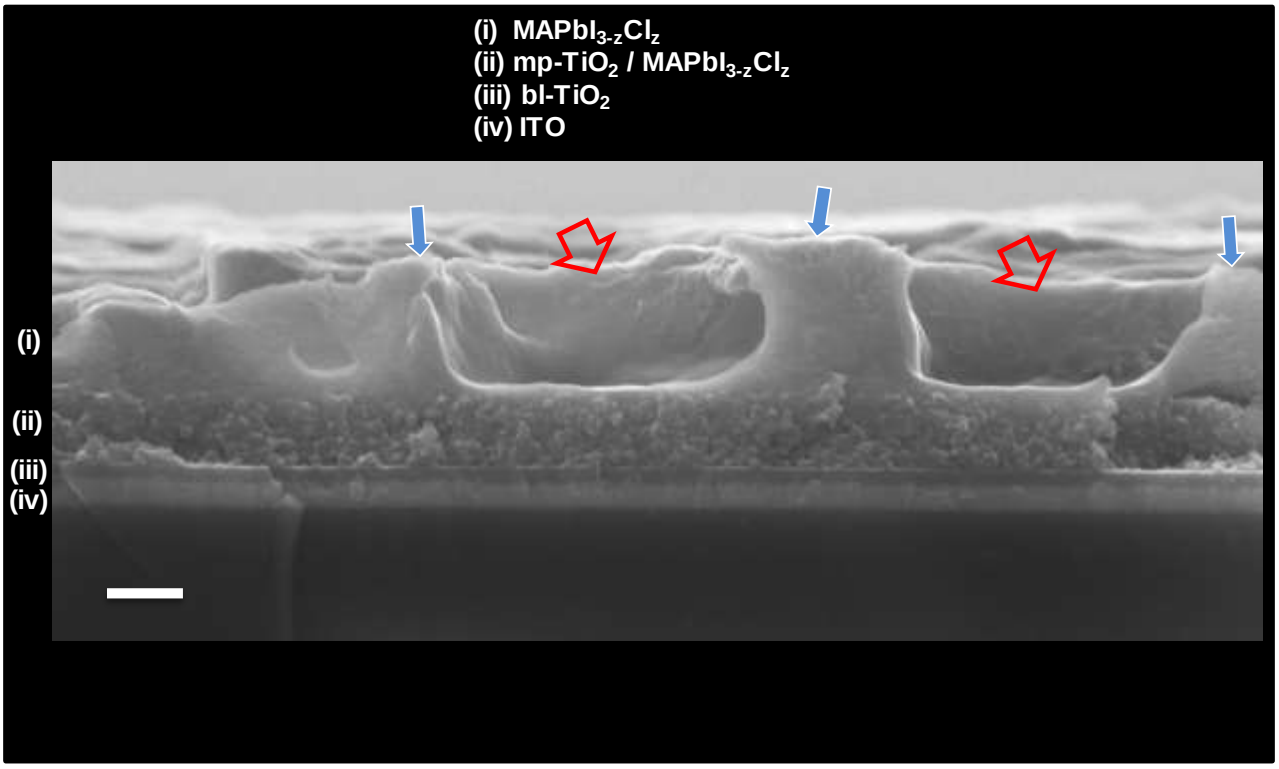

Figure S6. SEM image for a MP37.5MG3.0 DIO film cross-section with two pores evident. The scale bar is 300 nm. The red and blue arrows highlight pores and walls respectively.

Relationship between pore wall thickness and microgel volume fraction in the composite films

In the following an equation is derived that describes the relationship between the DIO wall thickness (W) and the volume fraction of MG in the composite film (ϕ_{MG}). The idealised geometry is shown in Fig. S7 at the point where the DIO film formed but before the MGs had collapsed. To derive the equation we first define the ϕ_{MG} in terms of the microgel volume and total volume of the parallelogram of height H (i.e., a cuboid) shown in the figure. These volumes are V_{MG} and V_{Cub}, respectively. Equations for the latter two volumes are then derived. The equations are then rearranged to obtain an equation for W in terms of the MG diameter (D) and ϕ_{MG}. The final equation is then tested in limiting forms to verify its correctness.

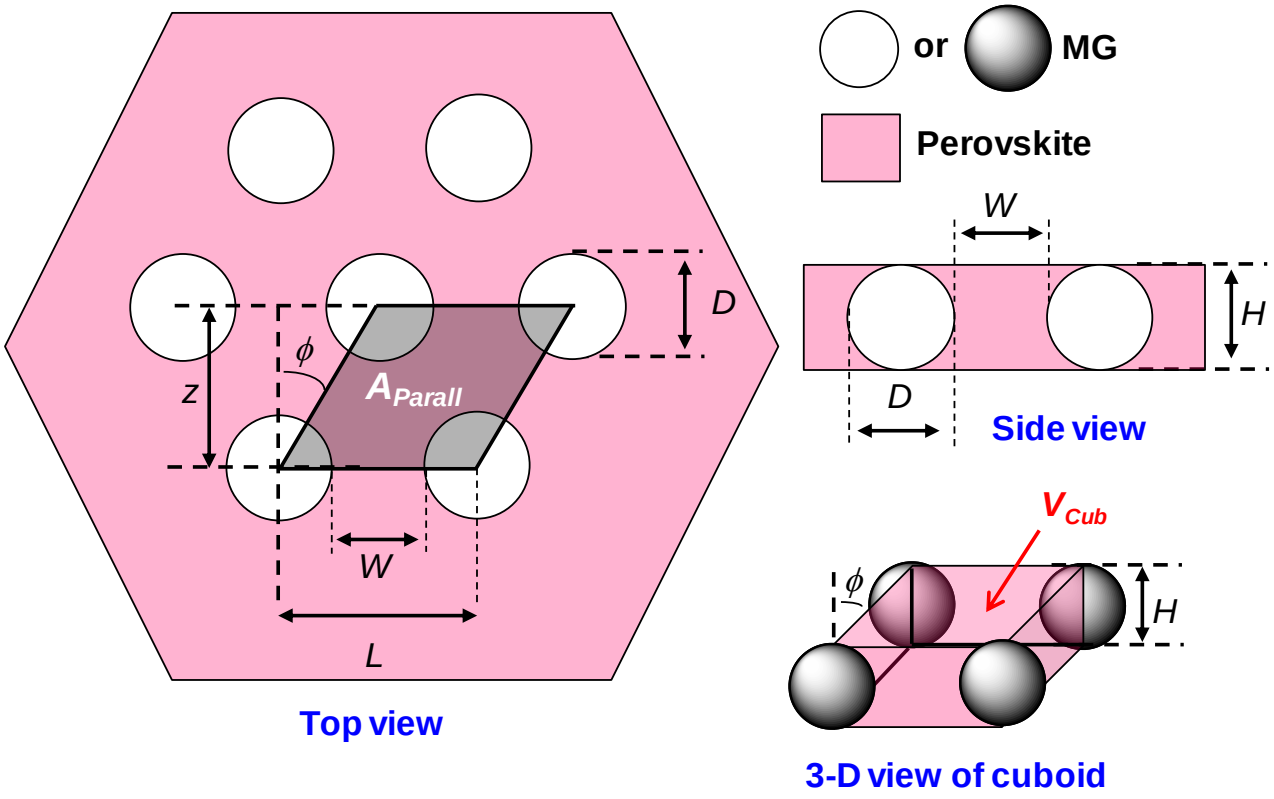

Figure S7. Idealised geometry of MGs within a perovskite film viewed from the top and side before the MGs had collapsed. The angle ϕ is 30°. A_{Parall} and V_{Cub} are the area and volume of the parallelogram and cuboid, respectively. They are related by: $V_{Cub} = HA_{Parall}$.

The following assumptions are used. The value of ϕ_{MG} for the film is the same as that of the cuboid defined in the figure and the perovskite that forms within the underlying meso-TiO_2 layer is

neglected. A hexagonal arrangement of the MGs is also assumed to be present, which is supported by the SEM images in Fig. 3A - C. It is also assumed that perovskite does not form inside the de-swollen MGs and that the mass ratio of perovskite to MG is maintained during spin coating. We further assume the perovskite precursors are fully converted to the final perovskite. The latter assumption is supported by the X-ray diffraction patterns in Fig. 6. It is further assumed that H is that of the MGs before they flattened and that the pore diameter (D_{Pore}) is the same as D and is constant. This latter assumption is not strictly correct as shown by Fig. 5B. However, the change in D_{Pore} is less than 35% for the systems studied.

The expression for ϕ_{MG} is simply $\phi_{MG} = V_{MG}/V_{Cub}$. There is one MG within each cuboid (i.e., four corner shared MGs). The equations for these two volumes are given by (S1) and (S2), respectively.

$$V_{MG} = \frac{\pi D^3}{6} \qquad \text{(S1)}$$

$$V_{Cub} = zLH = L^2 H cos\phi = \frac{\sqrt{3}}{2} L^2 H \qquad \text{(S2)}$$

Using $L = W + D$, and assuming $H = D$, then equation (S2) becomes:

$$V_{Cub} = \frac{\sqrt{3}}{2} D(W + D)^2 \qquad \text{(S3)}$$

Using the equation for ϕ_{MG} (above) and rearranging to solve for W gives the following equation.

$$W = D\left\{\left(\frac{\pi/(3\sqrt{3})}{\phi_{MG}}\right)^{1/2} - 1\right\} \qquad \text{(S4)}$$

The value $\pi/(3\sqrt{3}) = 0.605$ corresponds to the packing fraction of 2-D hexagonal close packed spheres, which is termed here as $\phi_{MG(hcp\text{-}2D)}$. Hence,

$$W = D\left\{\left(\frac{\phi_{MG(hcp-2D)}}{\phi_{MG}}\right)^{1/2} - 1\right\} \qquad \text{(S5)}$$

Equation (S5) shows that $W \sim D$ (at fixed ϕ_{MG}), which is reasonable because the inter-MG separation will increase with D. Furthermore, the equation predicts that at $W = 0$, $\phi_{MG} = \phi_{MG(hcp\text{-}2D)}$

Relationship between absorbance and perovskite coverage of the surface

The following describes the derivation of an equation for the relationship between the absorbance of a DIO film and the fractional coverage of the meso-TiO_2/perovskite surface by the perovskite (θ_{MP}) in the capping layer (see Fig. S8). We first consider the dependence of absorbance (*Abs*) on the film thickness and absorption coefficient (α). Then an expression for the fractional coverage of the DIO film by perovskite ($\theta_{MP(DIO)}$) is given which uses the idealised geometry given in Fig. S7 and Fig. S8. After considering the fractional coverage of the surface by the DIO film (θ_{DIO}) an equation for θ_{MP} is obtained which is related to *Abs* and is then tested for limiting cases.

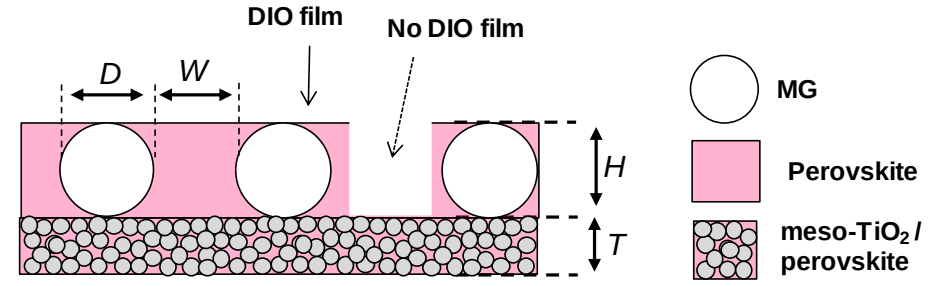

θ_{DIO} = Fractional coverage of meso-TiO_2 / perovskite by the DIO film
$\theta_{MP(DIO)}$ = Fractional coverage of DIO film by perovskite
θ_{MP} = Fractional coverage of meso-TiO_2 / perovskite surface by capping layer perovskite

Figure S8. Idealised geometry of MGs within a perovskite film viewed from the side before the MGs had collapsed. The perovskite/MG composite film is the capping layer and sits on a perovskite/mesoporous TiO_2 layer with a thickness of *T*. The perovskite/MG becomes the DIO film when the MGs flatten. The incident irradiation for the UV-visible study is normal to the film plane.

The intensity of light at a distance *x* (i.e., *I(x)*) is related to the incident light intensity (*I(0)*) by[2],

$$I(x) = I(0)e^{-\alpha x} \qquad \text{(S6)}$$

where α is the absorption coefficient. Combining equation (S6) with $Abs = -log(I(x)/I(0))$ leads to *Abs* = (αx)/2.303. The absorbances for the capping layer (thickness, *H*) and mesoporous layer (thickness, *T*) are assumed to be additive, i.e.,

$$Abs = Abs_{cap} + Abs_{meso} = \frac{\alpha_{cap} H}{2.303} + \frac{\alpha_{meso} T}{2.303} \qquad \text{(S7)}$$

where α_{cap} and α_{meso} are the absorption coefficients for the capping layer and meso-TiO_2/perovskite layer, respectively. It is further assumed that $\alpha_{meso}T$ is constant because the meso-TiO_2 layer thickness was constant (250 nm) and that sufficient perovskite was present to fill that layer.

The parameter α_{cap} will increase with increasing θ_{MP} reaching the value for perovskite (α_{MP}) when θ_{MP} = 1.0. Hence,

$$\alpha_{cap} = \theta_{MP}\alpha_{MP} \qquad \text{(S8)}$$

The value for θ_{MP} is also proportional to θ_{DIO} as well as the fraction coverage of perovskite within the DIO film ($\theta_{MP(DIO)}$), and therefore,

$$\theta_{MP} = \theta_{MP(DIO)}\theta_{DIO} \qquad \text{(S9)}$$

The measured θ_{DIO} values are given in Table S1. Considering the geometry shown in Fig. S7 (Top view) the following expressions apply for the areas of the MGs (A_{MG}) and 2-D parallelogram (A_{Parall}) in the plane parallel to the film surface. Note there is one MG per parallelogram.

$$A_{Parall} = L^2 cos\phi = \frac{\sqrt{3}}{2}(W + D)^2 \qquad \text{(S10)}$$

$$A_{MG} = \frac{\pi D^2}{4} \qquad \text{(S11)}$$

Furthermore, $\theta_{MP(DIO)} = 1 - \frac{A_{MG}}{A_{Parall}}$ (S12)

Equations (S10) and (S11) can be combined with equation (S12) to give

$$\theta_{MP(DIO)} = 1 - \frac{\pi}{2\sqrt{3}}\left(\frac{1}{1+{}^{W}/_{D}}\right)^2 \qquad \text{(S13)}$$

Using equations (S7) - (S9) and equation (S13) we can describe the variation of the absorbance based on the MG-dependent parameters *D* and *W* using

$$Abs = \frac{\alpha_{MP}\theta_{MP}H}{2.303} + Abs_{meso} \qquad \text{(S14)}$$

In the limit that *W* approaches zero, $\theta_{MP(DIO)}$ = 0.093 from equation (S13). This corresponds to touching MG spheres and both θ_{MP} and and *Abs* have minimum values. It follows from equations (S9), (S13) and (S14) that *Abs* increases with increasing *W* because $\theta_{MP(DIO)}$ also increases.

Table S1. DIO film morphology and pore size.

Film	D_{Pore} / nm[a]	W / nm[b]	ϕ_{MG}[c]	θ_{DIO}[d]	$\theta_{MP(DIO)}$[e]	θ_{MP}[f]
MP45MG2.0	988 ± 60	529 ± 184	0.154	1.00	0.62	0.62
MP30MG2.0	922 ± 83	394 ± 111	0.215	0.36	0.56	0.20
MP37.5MG3.0	939 ± 63	377 ± 153	0.247	1.00	0.54	0.54
MP30MG3.0	866 ± 79	296 ± 88	0.291	0.75	0.50	0.37
MP25MG3.0	657 ± 87	244 ± 56	0.330	0.34	0.52	0.17
MP30MG4.0	812 ± 69	226 ± 56	0.353	1.00	0.44	0.44

[a] Average pore diameter. [b] Average width of the pore walls obtained from SEM. [c] Volume fraction of MG (see equation 1). [d] Fractional coverage of surface by DIO. [e] Calculated coverage of perovskite within the DIO regions. [f] Calculated fractional coverage of perovskite in the capping layer.

Table S2. Intensity of the perovskite peaks from XRD patterns for various films.[a]

Film	Intensity / Counts			FWHM
	(110)	**(220)**	**(222), (310)**	**(Average)**
MP25	450 [0.276]	300 [0.354]	139 [0.315]	0.315
MP25MG3.0	2232 [0.236]	1912 [0.354]	1146 [0.315]	0.302
MP37.5	3998 [0.236]	1353 [0.236]	445 [0.354]	0.276
MP37.5MG3.0	5202 [0.118]	3555 [0.236]	1342 [0.433]	0.262
MP45	8874 [0.183]	4010 [0.306]	1519 [0.317]	0.268
MP45MG2.0	16209 [0.177]	4549 [0.118]	1530 [0.276]	0.190

[a] The numbers in brackets are the full width at half maximum values in degrees.

Table S3. Line of best fit parameters from absorbance data fitting[a]

Wavelength / nm	*m*	*c*	R^2
480	3.71	1.96	0.92
740	2.27	0.47	0.93
800	1.76	0.27	0.92

[a] Parameters for $Abs = m\theta_{MP} + c$.

Table S4. Solar cell performance data measured for various devices.

Devices	Cell no.	J_{sc} (mA/cm^{-2})	V_{oc} (mV)	FF (%)	PCE (%)
MP37.5MG3.0	1	20.00	819	40.8	6.68
	2	20.56	804	37.8	6.25
	3	29.3	830	34.3	8.35
	4	21.73	841	31.4	5.74
	5	19.88	800	35.3	5.61
	6	18.62	884	44.2	7.27
	7	14.06	850	50.6	6.05
	8	18.25	855	42.8	6.68
	9	18.08	828	42.0	6.29
	10	18.36	826	45.6	6.92
	Average	19.88 ± 3.89	834 ± 25	40.5 ± 5.8	6.58 ± 0.81
MP37.5	1	20.08	832	24.5	4.09
	2	19.99	808	27.5	4.44
	3	12.91	842	42.6	4.63
	4	11.23	797	44.2	3.95
	5	14.54	713	47.9	4.97
	6	24.82	813	30.5	6.15
	7	14.34	811	48.1	5.59
	8	14.10	809	48.1	5.48
	9	13.87	736	43.2	4.41
	Average	16.21 ± 4.41	795 ± 43	39.6 ± 9.5	4.86 ± 0.75

References

1. M. Chen, M. Z. Mokhtar, E. Whittaker, Q. Lian, B. Hamilton, P. O'Brien, M. Zhu, Z. Cui, S. A. Haque, and B. R. Saunders. *Nanoscale* 2017, **9**, 10126-10137.
2. J. Nelson. *The physics of solar cells, Imperial College London Press, London.* 2007.